Lawrence Berkeley Laboratory
UNIVERSITY OF CALIFORNIA

Materials & Chemical Sciences Division

National Center for Electron Microscopy

To be presented at the ISIAT '90, Tokyo, Japan, June 4–8, 1990 and to be published in the Proceedings

Transmission Electron Microscopy Study of ICB Al on Ge and Si{001} Substrates

U. Dahmen and K.H. Westmacott

April 1990

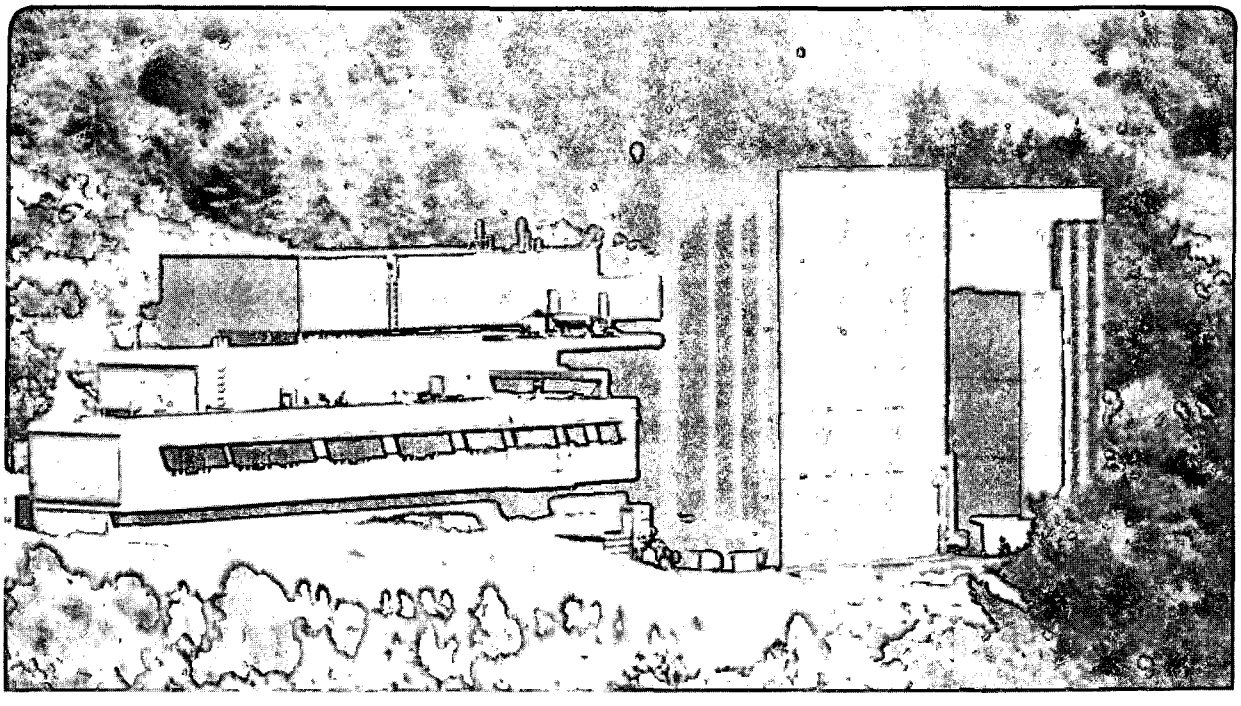

Prepared for the U.S. Department of Energy under Contract Number DE-AC03-76SF00098.

DISCLAIMER

LBL-29034

TRANSMISSION ELECTRON MICROSCOPY STUDY OF ICB Al ON Ge AND Si {001} SUBSTRATES

U. Dahmen and K.H. Westmacott

Materials & Chemical Sciences Division
National Center for Electron Microscopy, Lawrence Berkeley Laboratory
University of California, Berkeley, CA. 94720

ISIAT'90, Tokyo, Japan 6/4-6/8/90 and to be published in the proceedings

This work was supported by the Director, Office of Energy Research, Office of Basic Energy Sciences, Material Sciences Division of the U.S. Department of Energy under Contract No. DE-AC03-76SF00098.

TRANSMISSION ELECTRON MICROSCOPY STUDY OF ICB Al ON Ge AND Si {001} SUBSTRATES

U. Dahmen and K.H. Westmacott

University of California, National Center for Electron Microscopy,
Lawrence Berkeley Laboratory, Berkeley, CA 94720

1. Introduction

Ionized Cluster Beam (ICB) deposition is a novel technique for the production of thin films with interesting and unusual structures and properties. Its development effort has been spearheaded at Kyoto University [1], but interest in the technique has become widespread in recent years. At Berkeley, research is underway to characterize and understand the structure of interfaces in such films. Transmission electron microscopy (TEM) is being employed to obtain images of the atomic structure and the defects typical for these materials with the aim of understanding the relationship between deposition conditions and the structural characteristics of such interfaces {e.g. 2]. A question of fundamental importance in the formation of high-quality films is how the crystal structures of the substrate and the overlayer affect the epitaxial orientation relationship between them. In this study we present a comparison between Al films grown on two different substrates: {001} Si and {001} Ge. The interface structures are characterized in plan view by conventional microscopy using diffraction and moiré contrast and in cross section by high resolution microscopy. Thin films of Al grown on {001} Si are found to be distinctly different from Al films grown on {001} Ge substrates. The relationship between interface structure and film growth is discussed by comparison with interfaces produced by precipitation reactions in Al-Si and Al-Ge alloys.

2. Experimental

Specimens for electron microscopy were made from samples of ICB-deposited aluminum on {001} germanium and {001} silicon prepared at the Kyoto Ion-Beam Engineering Laboratory, by well established procedures. For plan view observations 3mm diameter discs were cut from the substrate and back-thinned to electron transparency from the substrate side by mechanical dimpling, followed by ion-beam thinning. With the preparation technique used, the plan view TEM specimens consisted of the freestanding ICB Al (wedge-shaped in cross section) near the hole at the center of the disc. Further away from the hole the Al remained supported by the silicon substrate. Cross-sectional TEM specimens were prepared by cutting the ICB wafer into thin (1mm) strips, turning them on edge and gluing them together to form composite sandwiches of the substrate and deposited film layers. Three millimeter TEM discs were cut from the sandwiches and thinned to electron transparency using standard mechanical dimpling and ion-beam milling techniques [see e.g. 3. The wafer strips can be cut in different crystallographic directions to optimize the subsequent high resolution imaging conditions and to provide orthogonal views of the interface structures. By relating the observations

to plan view images of the specimen, models of the deposited film and its interface with the substrate and with other orientation variants can be constructed.

The high resolution microscopy was performed on the JEOL 1000 Atomic Resolution Microscope with a point resolution of 1.6 Å operated at 800 kV. In-situ studies were performed on the Kratos EM 1500 operated at 1500 kV. This microscope is equipped with a lens-coupled 80mm, low light level, high-resolution Westinghouse TV camera used with a YAG scintillator, and a double tilt, 750°C side entry heating rod. Conventional contrast experiments were conducted on a standard 200 kV microscope.

3. Experimental Results

3.1. Orientation Relationships

Fig. 1 compares diffraction patterns from Al after ICB deposition on {001} Ge and Si. In both cases the incident beam is normal to the substrate, i.e. the orientation is that of a plan view sample. The difference is clearly apparent: on a Ge substrate, Al forms in a single orientation variant of the so called Bain orientation relationship [4] whereas on a Si substrate Al deposits in two orientation variants of the inverse Bain relationship [e.g.5]. Both are orientation relationships of high symmetry, and Fig. 2 illustrates them schematically. From the schematic it is clear that the difference between the two cases is simply a 45° rotation about the face diagonal of the substrate crystal structure. In both orientation relationships the film has only one direction in common with the substrate. On Ge, this is the <100> direction normal to the substrate whereas on Si this is a horizontal <110> direction in the plane of the substrate. Crystallographically, the only difference between the two situations is a change of 4% in the lattice parameter of the substrate: $a_{Ge} = 5.65$ Å, $a_{Al} = 5.43$ Å. It is surprising to find that as a result of this small difference, Al films on {001} Ge form {001} single crystals but Al films on {001} Si form {110} bicrystals.

The Bain orientation relationship observed on Ge, illustrated in Fig. 3, is easier to understand than the inverse Bain relationship found on Si. The atomic arrangement in Ge, when projected onto the {001} plane of the substrate is metrically very similar to that of Al. Notice how the Al unit cell is rotated relative to the Ge cell by 45° about the <001> projection axis; this defines the Bain orientation relationship. The corresponding cells in the two structures are therefore not the face centered cubic unit cells of each with a mismatch of 37 % but a the cubic unit cell of the Al lattice with an inscribed tetragonal cell of the Ge. In the metallurgy of steel this is known as the Bain correspondence [e.g. 6]. With this orientation the mismatch between the lattices is measured along corresponding directions, here $110_{Ge} \parallel 100_{Al}$, with only -1.1 % mismatch at room temperature. Furthermore, this mismatch decreases with increasing temperature due to the differential thermal expansion of the two materials. The small magnitude of this mismatch is reflected in the electron diffraction pattern which is almost identical to that of a single crystal. The effect of the lattice mismatch is only apparent in the fine structure of the diffraction spots.

The same lattice correspondence could in principle occur on a Si substrate, but the mismatch would then be about -5% %. Apparently this is too large to maintain this correspondence. Instead, the Al lattice is rotated through 45° to the inverse Bain orientation shown in Fig. 2b. For comparison with the case of a Ge substrate, this correspondence is shown in projection in Fig. 4. In the common <110> direction the mismatch is large if a one-to-one correspondence is assumed. However, it can be seen that with a 4:3 correspondence the residual mismatch is less than 1 %. Fig 4 shows only one of the two orientation variants of Al that form on an {001} Si substrate. As they are rotated 90° relative to each other the two orientation variants on the Si substrate form a continuous bicrystal structure [7] with 90° tilt grain boundaries, whereas the single orientation variant on Ge leads to a single crystal Al film.

3.2. Plan View Microstructure

The difference between the two types of epitaxy on Ge and Si is also apparent in the microstructure of the Al films. Both structures show a wealth of interesting microstructural information. Fig. 5a shows a typical microstructure of an Al film on a Ge substrate. In this plan view sample the Ge has been partially removed at the bottom of the figure. In this region, inclined dislocations are clearly visible in the freestanding Al film. In the upper part of the micrograph, the Ge substrate forms an interference, or moiré pattern with the Al lattice. This pattern gives a magnified view of the distortions in the two overlapping crystal lattices. The spacing of parallel moirés is about $a^2/\Delta a$. Since for the Bain correspondence the mismatch $\Delta a/a$ between Al and Ge in the common {001} plane is about 1%, the magnification factor is about 100. Thus, although the moiré pattern appears highly distorted the real lattice distortions are 100 times smaller. The crossed moiré pattern in Fig. 5a was recorded under bright field conditions in exact <001> zone axis orientation. A simpler image is obtained after tilting the crystal into a two-beam orientation and recording a dark field image. This is shown in Fig. 5b where only one set of moiré fringes appears in the region of overlap between Al and Ge. The inclined dislocations in the Al film are now equally visible in the freestanding and the overlapping Al. The moiré pattern always remains perpendicular to the diffraction vector, a sign that the fringes are not in fact interface dislocations. Thus, the observed localized elastic distortions are due to inclined dislocations rather than a network of interface dislocations as is often found in heterophase interfaces.

Moiré fringe patterns are also observed in Al films on Si substrates but, as seen in Fig. 6 there are two types of linear array rather than one set of crossed fringes. Each linear array defines an orientation variant and the network of the continuous bicrystal structure can easily be seen through this contrast mechanism. The origin of these moiré fringes is the same as that in Al on Ge, i.e. interference between 200_{Al} and $220_{substrate}$ reflections. However, because the mismatch between these directions is four times larger for a Si substrate than for a Ge substrate, the moiré fringe spacing is four times smaller (inverse to the mismatch). The micrograph in Fig 6 is thus shown at higher magnification. Again, there is no indication of interface dislocations between the Si substrate and the Al film and extensive contrast experiments have confirmed the absence of any localized elastic reaction.

3.3. High Resolution and In-situ Observations

The nature of the interface between the substrate and overlayers is of fundamental importance in understanding both the growth and properties of ICB films. High resolution electron microscopy on cross-sectional ICB samples provides a direct means for determining the atomic structure of not only this heterophase substrate/overlayer interface, but also the homophase interfaces between different grains in the overlayer. High resolution images also provide information on the magnitude and distribution of residual elastic stresses in ICB films. As discussed earlier, these stresses, which can arise from residual structural mismatching in epitaxially grown films, or from differential thermal contraction during cooling after an annealing treatment, can lead to distortions of the structure and affect important properties of the film.

A technique for graphically displaying the presence of elastic strains in high resolution images has recently been demonstrated [8]. Advantage is taken of the interference effects that were seen to lead to moiré patterns when two crystal overlap along the beam path (see for example Fig. 5). The same effect can be used to form composite images from high resolution micrographs and display the continuous small changes in lattice parameter corresponding to the elastic strain field. Since an atomic resolution image is a direct representation of the periodic crystal structure of the sample, the superposition of such a micrograph with a standard reference grid of suitably chosen (different) lattice parameter will result in the formation of a moiré pattern. Using this technique it is possible to reveal imperfections produced by elastic strains and defects such as dislocations in high resolution images of crystalline materials.

All of these techniques are being applied in the analysis of the Al/Ge and Al/Si ICB structures. Typical high resolution images of the structure at the heterophase interface between (100) Al and (100) Ge are shown in Figure 7. The cross-section is tilted so that a <100> zone axis in the Al is precisely parallel to a <100> in the Ge to allow resolution of the atomic structure up to, and at, the interface (compare crystallography with Figure 2a). It is apparent in figure 7a that in some regions the interface is planar to a level of one atomic spacing. Elsewhere, a roughening of up to four planar spacings in extent is evident (see Figure 7b). Some caution is necessary in making this interpretation, however, since uneven ion-beam milling, due to differential sputtering rates, can lead to image artifacts. Overall it is safe to say that the interfaces are relatively flat and no direct evidence is found indicating atomic interdiffusion of the Al and Ge (at least in the as-deposited films). Similar results have been found for Al/Si ICB films [9].

An illustration of the use of the moiré effect to produce a magnified pattern of elastic strain distribution is given for the cross section of Al on {001} Ge in Figure 8. In this example, very little distortion of the pattern is seen in either the Al or Ge lattices. This is a direct and unambiguous indication that both the substrate and overlayer lattices remain rigid right up to the interface, and that no relaxation of the structure has occurred. This may be confirmed by referring to the schematic diagrams of the three possible interface structures shown in Figure 9.

The rigid (unrelaxed) structure (Figure 9a) results in two separated undistorted moiré patterns joined at the interface. An elastically strained interface, 9 (b), would given rise to a moiré that is continuous across the interface; finally, a structure in which the strain is relaxed by the introduction of a periodic array of misfit dislocations, 9c, would be revealed by the presence of dislocations in the Al moiré pattern. The fact that the moiré pattern observation eliminates Fig 9b and c as possibilities directly confirms the findings of the plan view observations on the specimen described in Section 2 that no dislocations are present in the heterophase interface.

Figure 10 is a high resolution image from a cross section of Al on {001} Si showing both heterophase and homophase interfaces. The heterophase interface is again planar to within one atomic spacing and there is no evidence of interdiffusion even at the most susceptible location - the triple boundary where the Al bicrystal and Si substrate meet. Since the specimen was prepared in the as-deposited condition the Al bicrystal homophase interface (seen normal to the Al/Si interface) has not yet adopted its lowest energy planar configuration. Nevertheless, the two orientation variants of the Al lattice are clearly visible and the continuity of the common {110} planes across the grain boundary can be used to detect whether a rigid body shift parallel to the growth direction exists between the Al grains. Careful measurements on this high resolution micrograph have shown that within experimental error the lattices are in exact registry in this direction [8].

It is worth emphasizing that in this system of {110} Al on {001} Si, the orientation relationship of the Al bicrystal is such, (see Figure 2b), that imaging in a cross-sectional specimen, an Al grain boundary in a <110> direction of the Si substrate permits both (orthogonal) views of the Al structure to be obtained at the same time. This allows a three-dimensional atomic model of the structure to be constructed.

As a final example of the value of cross-sectional TEM imaging, consider the conventional micrograph shown in Fig. 11 of a {110}Al/{001}Si interface taken following in-situ heating for one hour at 400°C in the HVEM. Several interesting features are present in this micrograph. In spite of clear changes in the microstructure that have occurred during the annealing, the Al/Si interface has remained remarkably planar. The junctions of the bicrystal boundaries with the silicon show no evidence that diffusion of silicon along the Al boundaries has occurred. Similarly, no spikes of Al into the Si substrate are found. The appearance of a damaged zone 250 Å wide in the Si near its interface with the Al may be an indication of the uniform interdiffusion of Al and Si. The features in this zone, displaying black/white contrast, may be small point-defect clusters formed by irradiation of the specimen with electrons during the observation at 1.5 MeV. Localization of the damage near the interface could be explained by the presence of Al dissolved in the Si causing an increase in the damage cross-section and a higher production rate of point defects in the region. However, the observation of the damage free zone displaying fringe contrast immediately adjacent to the interface is not readily explained.

Assuming Al has diffused 500 Å into the Si during the 1 h anneal at 400°C, the diffusion coefficient D would be approximately 7 x 10^{-15} cm^2 s^{-1}. The literature does not contain diffusion data for Al in Si to assess whether this is a realistic value for D. Further work will be required to understand fully the origin of this effect. It is, however, interesting to note that preliminary observations on similarly annealed (111) Al / (111) Si films have not shown similar effects.

4. Discussion

The observations reported in this study pose an interesting fundamental question: if there is no apparent evidence of elastic relaxation at the interface then what type of interaction leads to the epitaxial alignment between the semiconductor substrate and the metal overlayer? It has been postulated that mismatch is important in determining the type of alignment in heteroepitaxial growth [10]. If lattice mismatch does in fact control epitaxial alignment, then why is there no apparent attempt at its accommodation by introducing interface dislocations? Experiments on different combinations of metal films and semiconductor substrates [11,12,13] have shown that deposition conditions, surface reconstruction prior to deposition, miscut and stacking fault energies may all play important roles in the delicate balance that determines heteroepitaxial alignment.

These questions are identical to those encountered in the study of the morphology and interface structure of Si or Ge precipitates in an Al matrix [5]. Careful experiments have shown that a number of different orientation relationships and interface facets are observed and even for large faceted precipitates no relaxations into a network of interface dislocations is found. Instead the two crystals are usually topotaxially aligned and exhibit atomically smooth facets that have the characteristics of an incoherent interface, i.e. one in which the two crystals behave as if they were mechanically joined with no atomic, elastic or diffusional interaction. However, clearly the bonding across the interface is strong enough to withstand substantial stresses during differential thermal expansion or mechanical deformation. The nature of these bonds and the resulting interface structure are at present unknown although theoretical studies suggest a change in the bonding environment with the degree of coverage during the intial stages of epitaxial growth [14]. It is possible that a very thin incommensurate layer forms between the two crystals, similar to the reconstructed layers that are found at some semiconductor surfaces or the incommensurate adsorbate layers in some physisorbed and chemisorbed systems [15]. However, if such a layer exists, it is very thin. Its detection by atomic resolution microscopy depends on the quality of samples and microscope resolution and must rely on computer image simulations of model structures. Efforts are currently underway to obtain a better answer to this fundamentally important question.

Acknowledgements

All the specimens for this study were provided by Prof. Yamada and his group at Kyoto University. This work was supported by the Director, Office of Energy Research, Office of Basic Energy Sciences of the U.S. Department of Energy under contract #DE-AC03-76SF00098.

Figure Captions

Figure 1: Transmission electron diffraction patterns from ICB films of single crystalline Al on {001} Ge (a), and bicrystalline Al on {001} Si (b). In (a), the Al and Ge are related by the Bain correspondence and the low index spots nearly coincide and are thus indistinguishable. In (b) two 110 Al patterns, superimposed on the 001 Si are outlined. Many additional spots arise from double diffraction.

Figure 2: Schematic diagrams comparing the orientation relationships between ICB Al on {001} Ge substrate (a), and {001} Si substrate (b). Only one of the two 110 orientations of the Al on Si is shown in (b).

Figure 3: Schematic diagram showing the interface atomic matching (c) between the Al (a) and Ge (b) in the correct relative orientation. The light shaded atoms represent atom positions with z-height of $\pm a/2$ in the Al and $\pm a/4$ in the Ge, while the darker shade corresponds to $\pm 3a/4$ in the Ge. In (c) the superposition of unshaded atoms corresponds to an exact match in positions, similar shaded atoms to an approximate match, and different shades to no match.

Figure 4: A schematic comparison of the atomic positions in one variant of the {110} Al (a) with the {001} Si (b) is shown in (c). The shading indicates different levels in the structure as in Figure 3.

Figure 5: Moiré patterns arising from interference of the electron waves in the single crystalline Al overlayer and Ge substrate. In the Bain orientation there is a 1% difference in the lattice spacing between 200 Al and 220 Ge. The micrograph in (a) was taken on the <001> zone axis, while (b) was tilted into a two-beam orientation with $g = 220_{Ge}/200_{Al}$.

Figure 6: Moiré patterns arising from interference between the Al overlayer and Si substrate reveal the Al bicrystal structure and elastic strains in the film.

Figure 7: Cross-sectional TEM micrographs from Al on {001} Ge showing regions where the interface is smooth (a) and more undulating (b).

Figure 8: Moiré pattern produced by superimposing a high resolution micrograph of the Al/Ge interface with a standard net indicating the absence of atomic relaxations at the interface. The moiré period in the Al is marked.

Figure 9: Schematic illustration of three possible interface structures; rigid (a), strained (b) and relaxed into periodic misfit dislocation array (c).

Figure 10: Cross section of a {110}Al/{001}Si specimen showing the triple-point junction of the Al bicrystal with the Si substrate.

Figure 11: Cross sectional conventional HVEM micrograph of a {110}Al/{100}Si specimen showing changes in the interface structure following a 1h in-situ anneal at 400° C.

References

1. I. Yamada, H. Inokawa and T. Takagi, J. Appl. Phys. 56, 2746 (1984)
2. K.H. Westmacott and U. Dahmen, Proc. ISIAT '89, 255 (1989)
3. MRS Symp. Proc. 115, J.C Bravman, R. Anderson and M.L. McDonald, eds. (1988)
4. E.C. Bain, Trans. Metall. Soc. AIME 70, 25 (1924)
5. J. Douin, U. Dahmen and K.H. Westmacott, Phil. Mag., in press
6. C.M. Wayman, "Introduction to the Crystallography of Martensitic Transformations", Macmillan, New York, (1964)
7. U. Dahmen and K.H. Westmacott, Scr. Met. 22, 1673 (1988)
8. C.J.D. Hetherington, U. Dahmen, M.A. O'Keefe, J. Turner, K.H. Westmacott, M.J. Mills and V. Vitek, MRS Symp. Proc. "HREM of Defects in Materials" (1990), in press
9. S. Tanaka, H. Usui, U. Dahmen, K.H. Westmacott and I. Yamada, Proc. ISIAT '89, 281 (1989)
10. A. Zur and T.C. McGill, J. Appl. Phys. 55, 378 (1983)
11. F.K. LeGoues, W. Krakow and P.S. Ho, Phil. Mag. A, 53 (1986)
12. F.K. LeGoues, M. Liehr and M. Renier, MRS Symp. Proc. 94, 121 (1987)
13. Z. Lilienthal-Weber, J. Vac. Sci. Techn. B 5, 1007 (1987)
14. J.S. Nelson, Inder P. Batra and C.Y. Fong, J. Vac Sci. Techn. A 6, 743 (1988)
15. A. Zangwill, "Physics at Surfaces", Cambridge Univ. Press, Cambridge (1988)

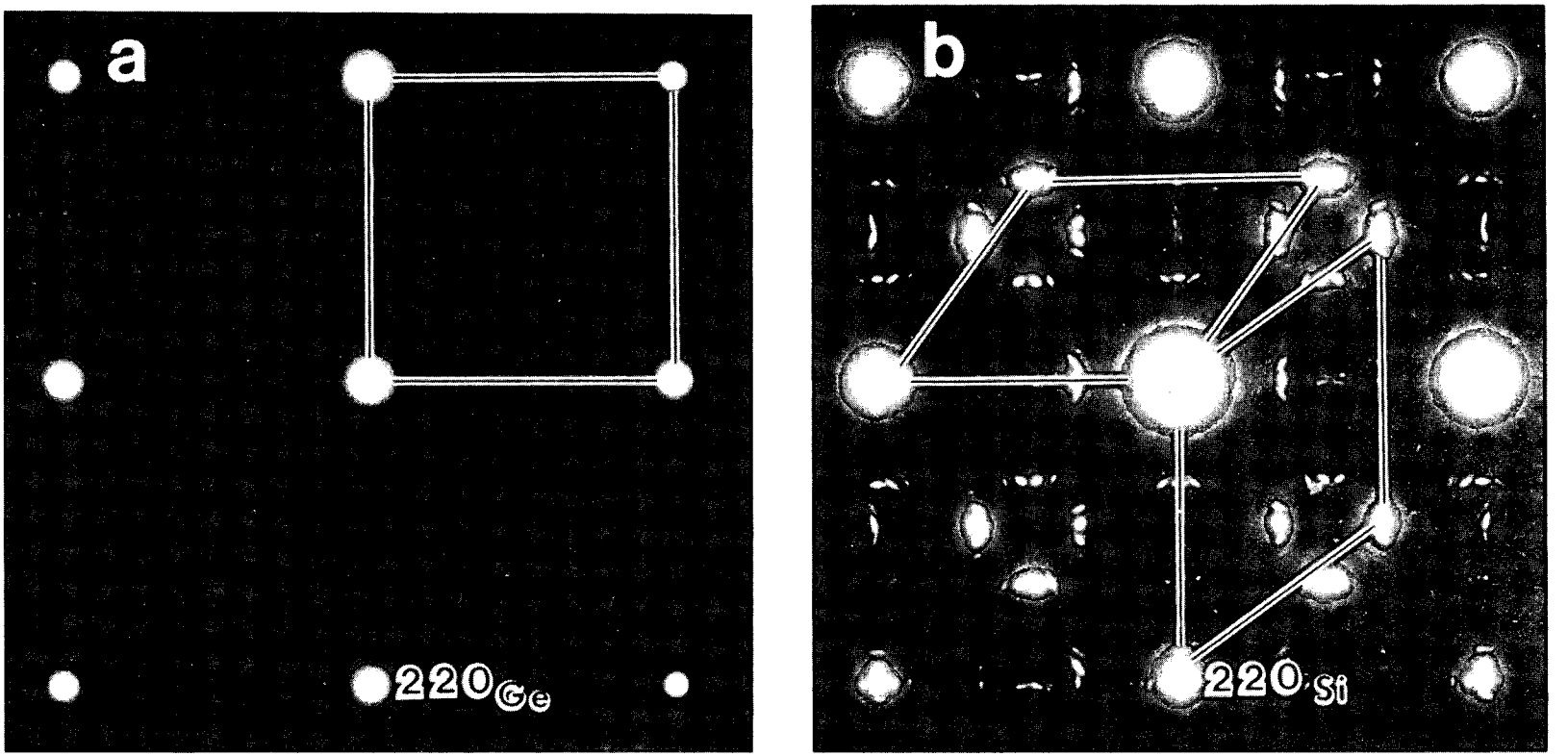

XBB 906-04597

Figure 1

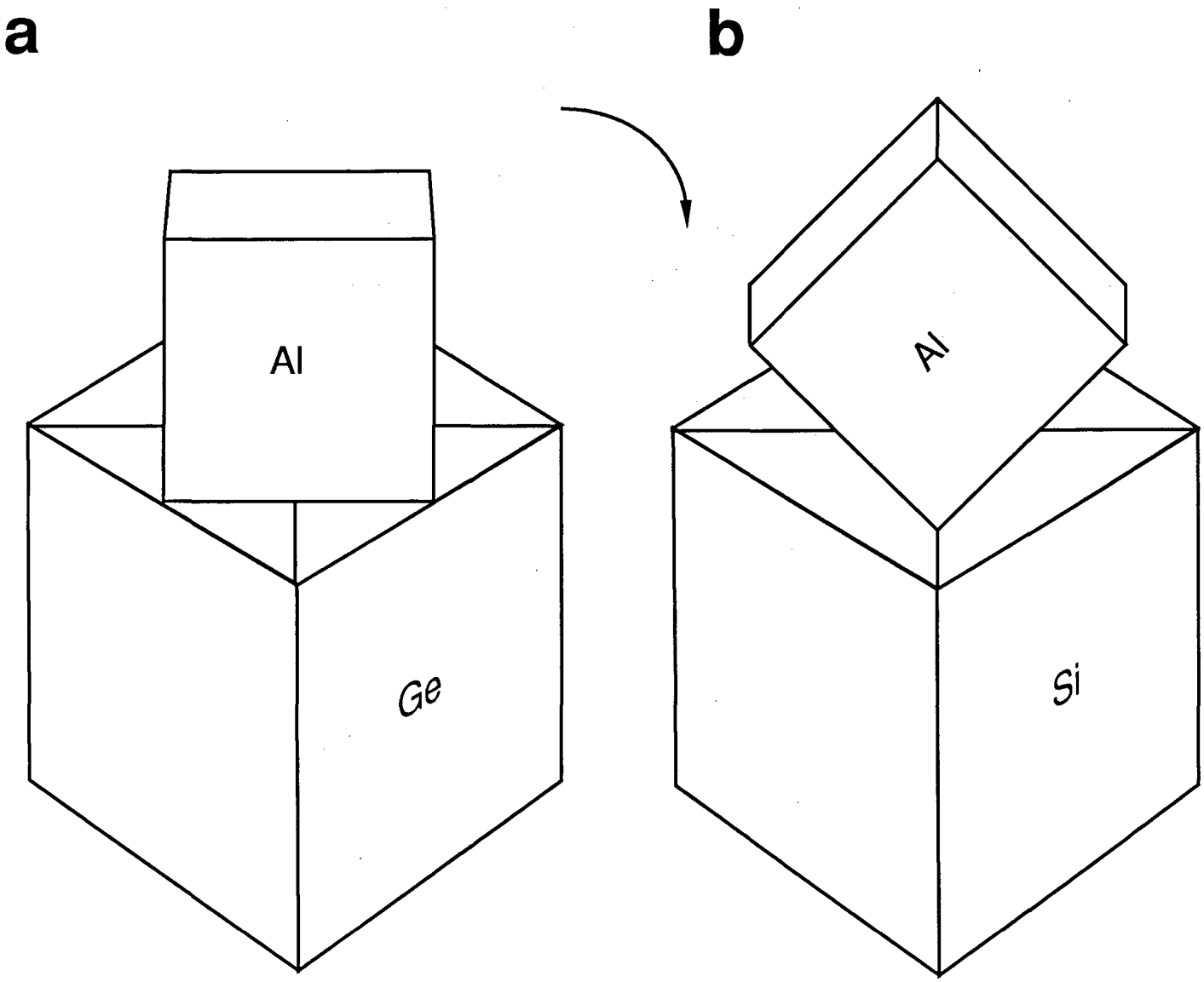

Figure 2

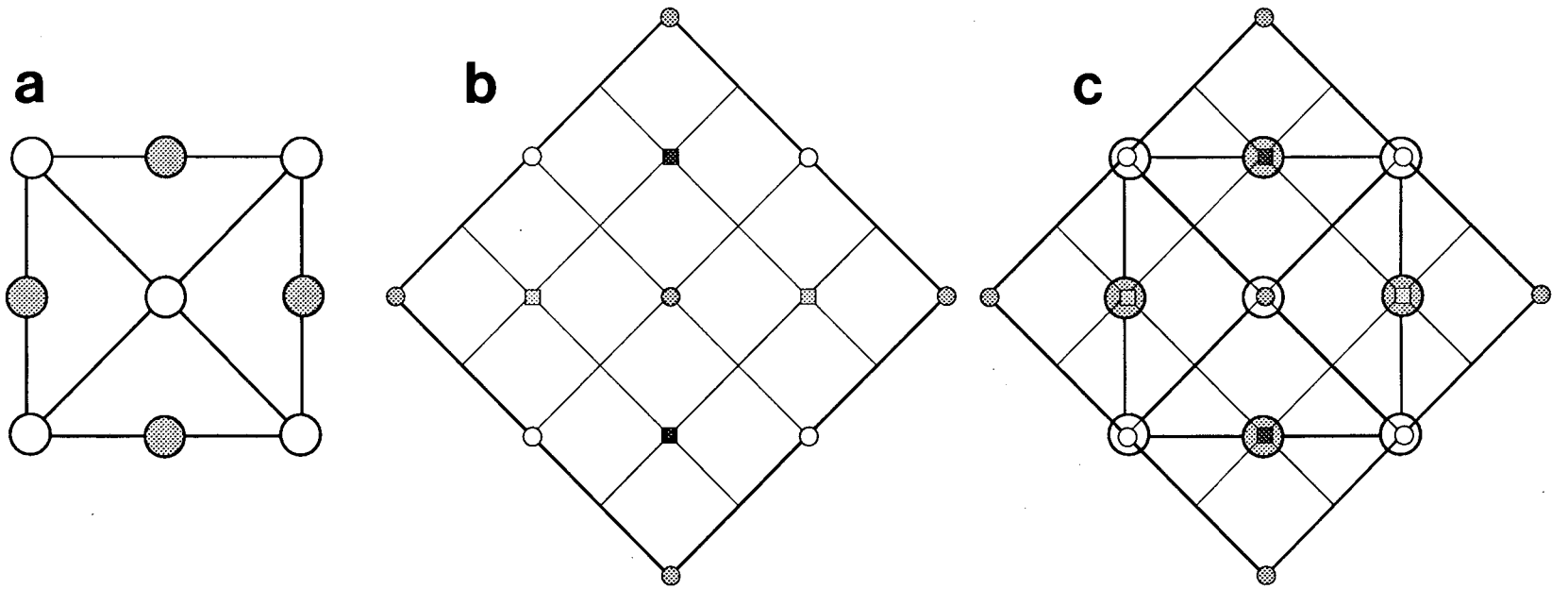

Figure 3

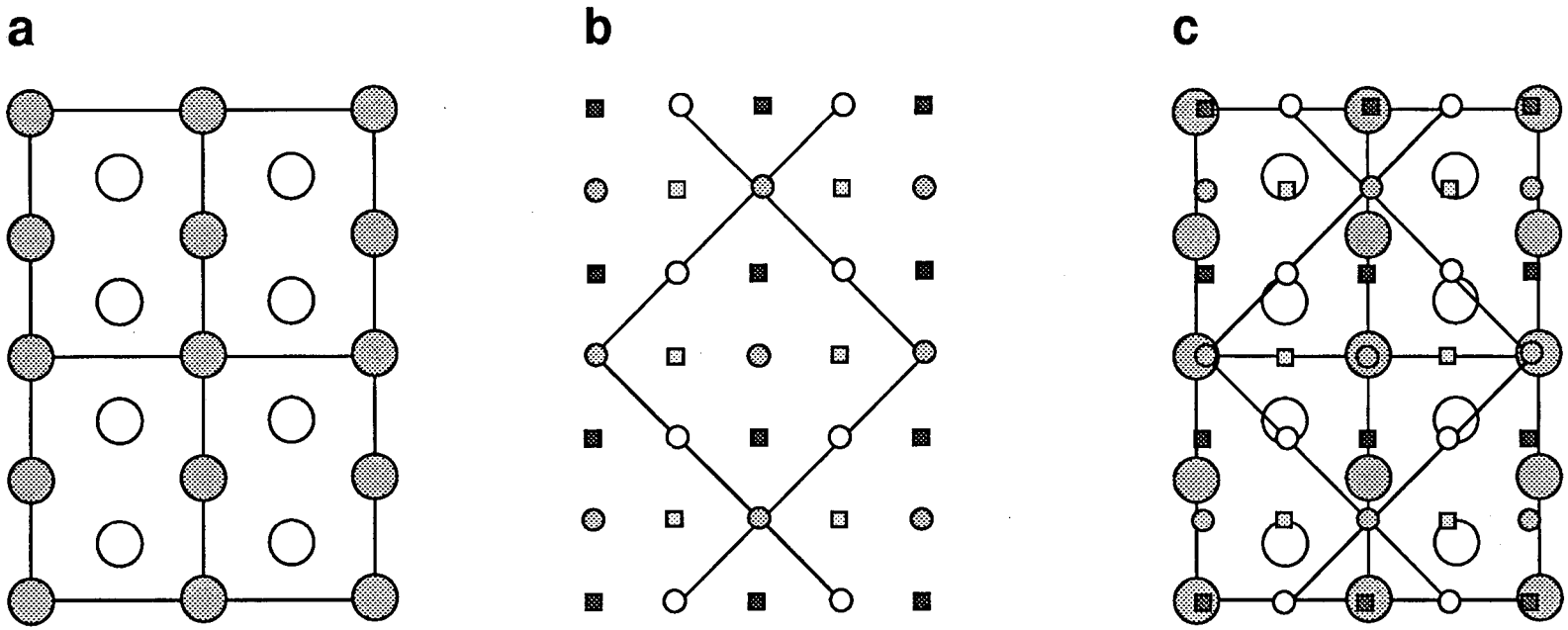

Figure 4

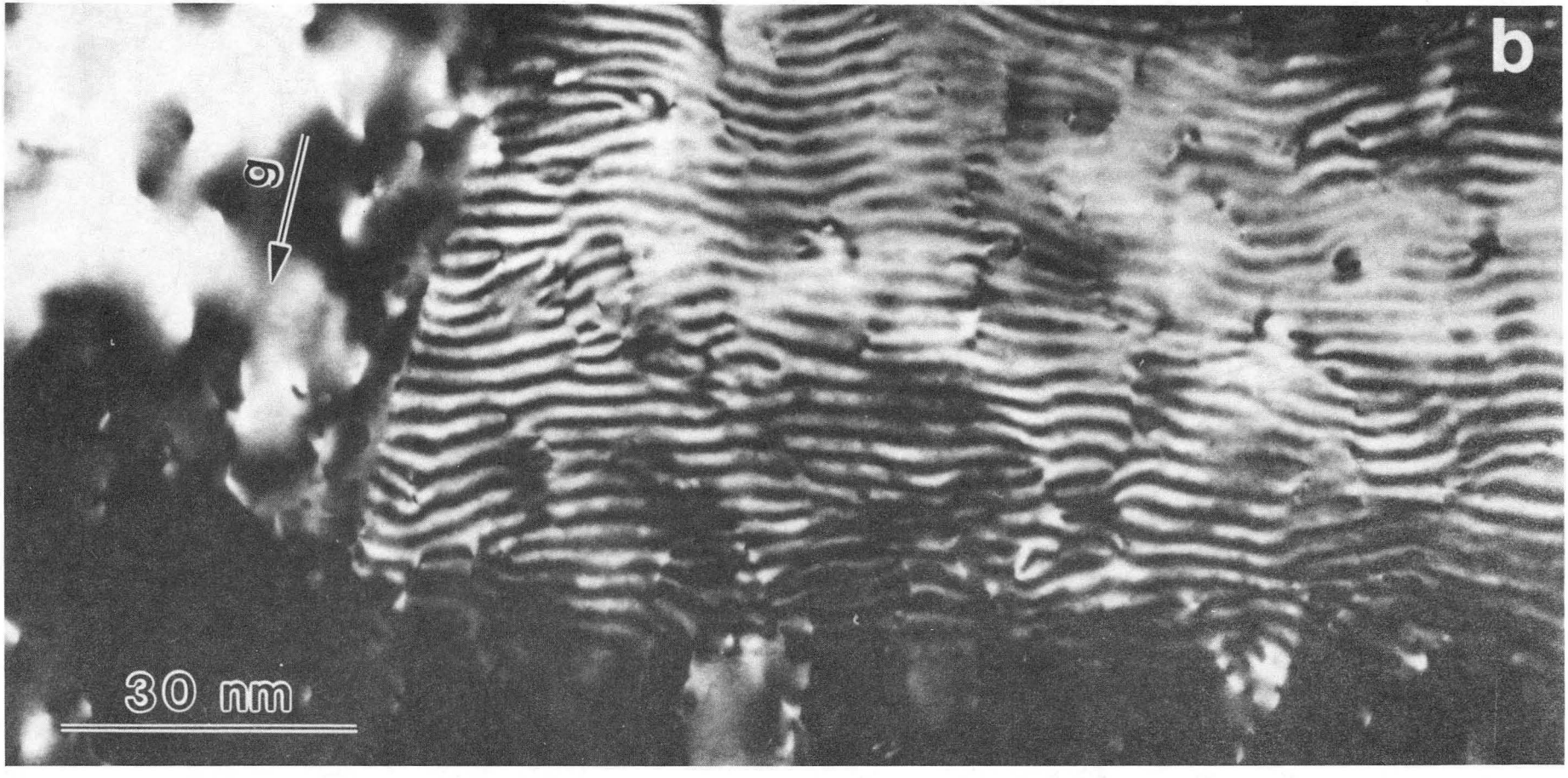

XBB 906-04593

Figure 5a

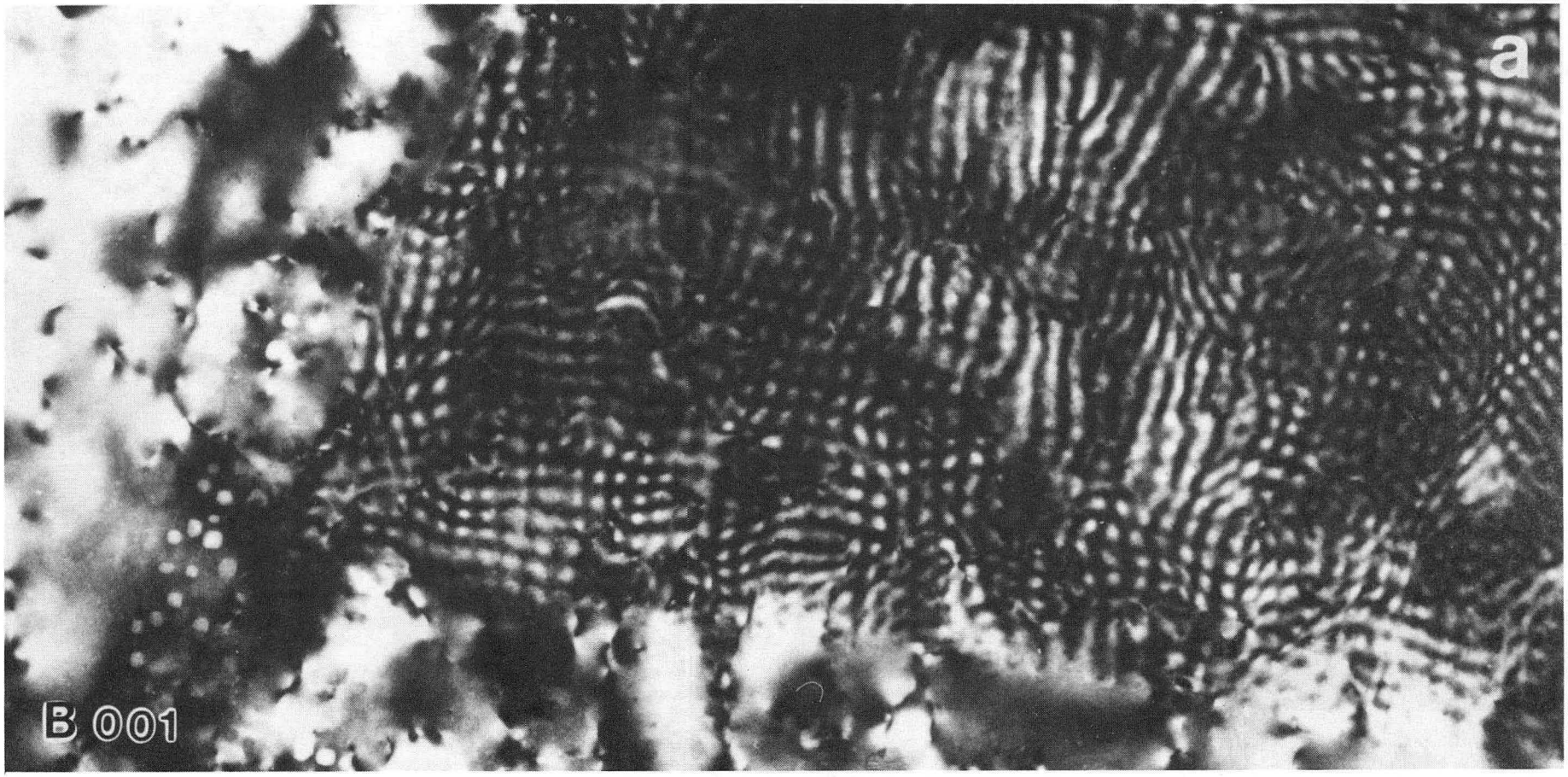

XBB 906-04593

Figure 5b

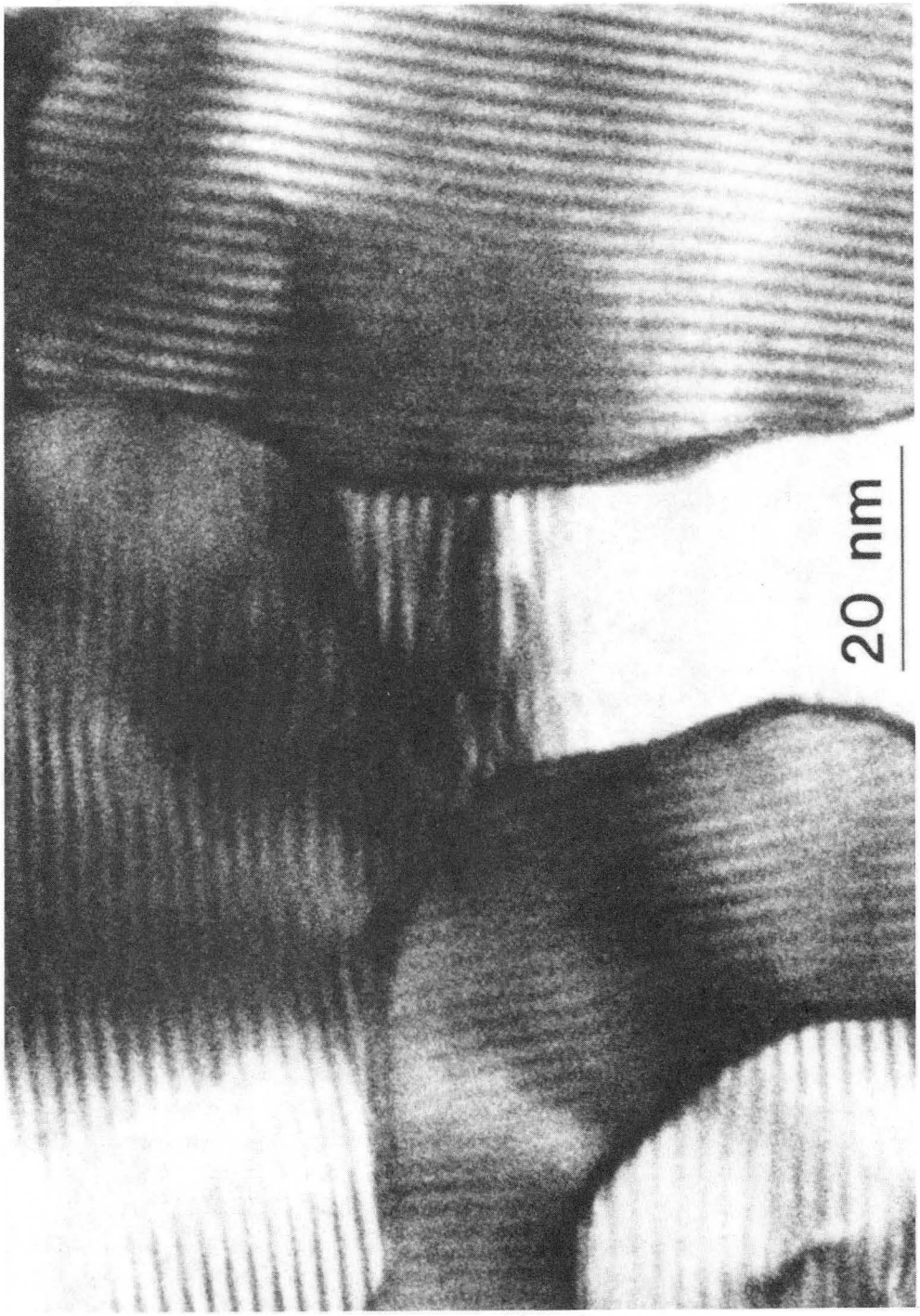

XBB 906-04598

Figure 6

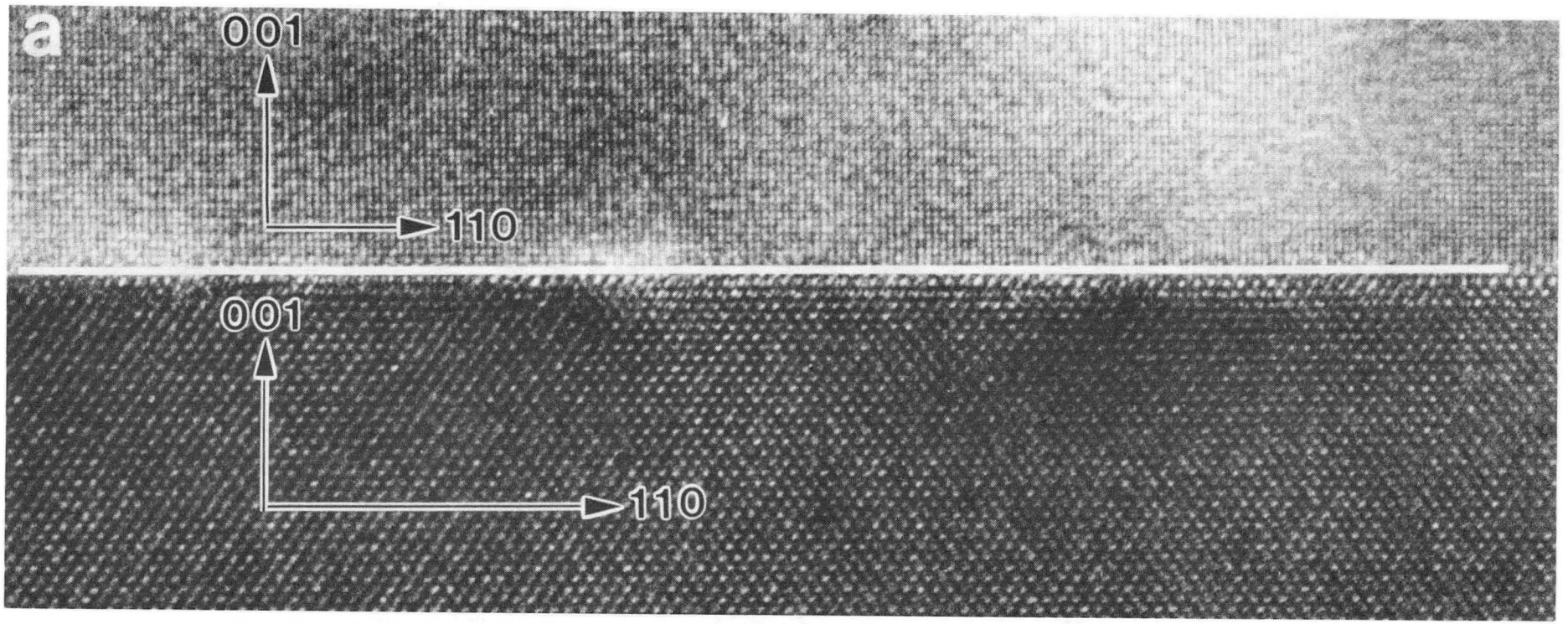

XBB 906-04592

Figure 7a

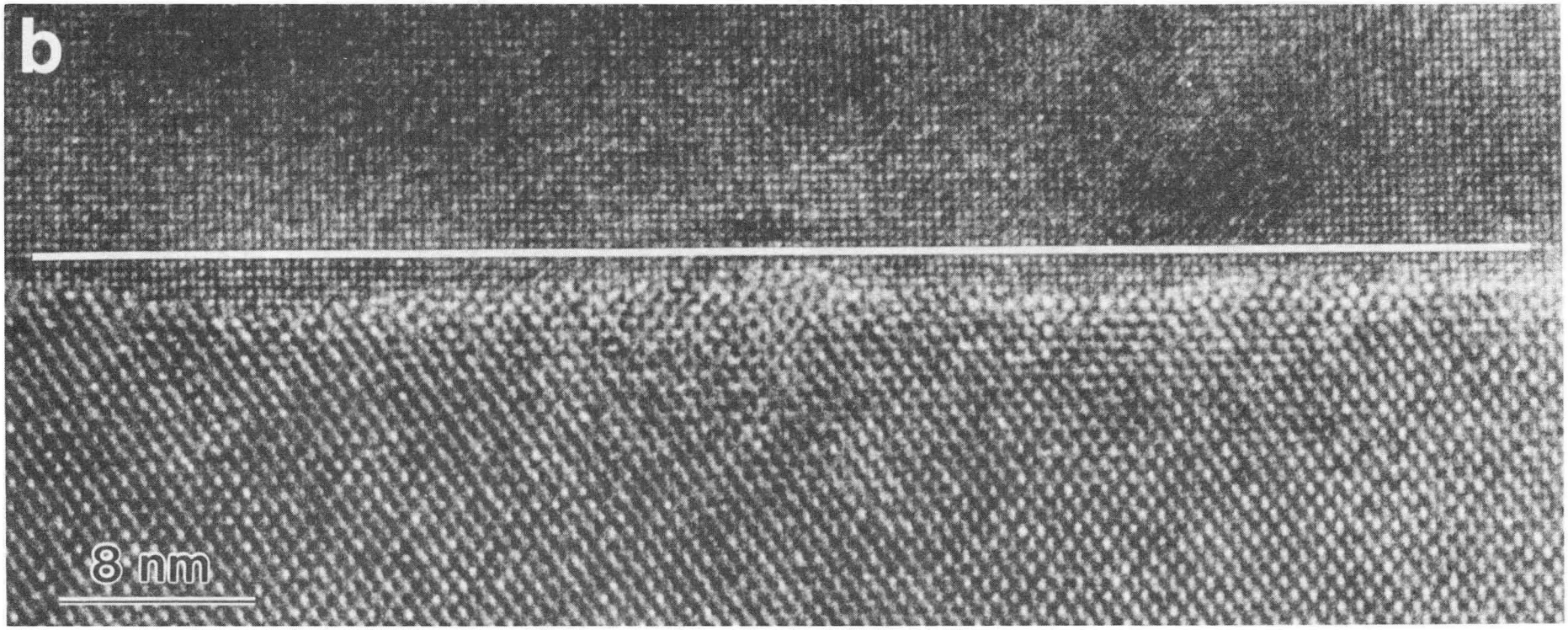

XBB 906-04592

Figure 7b

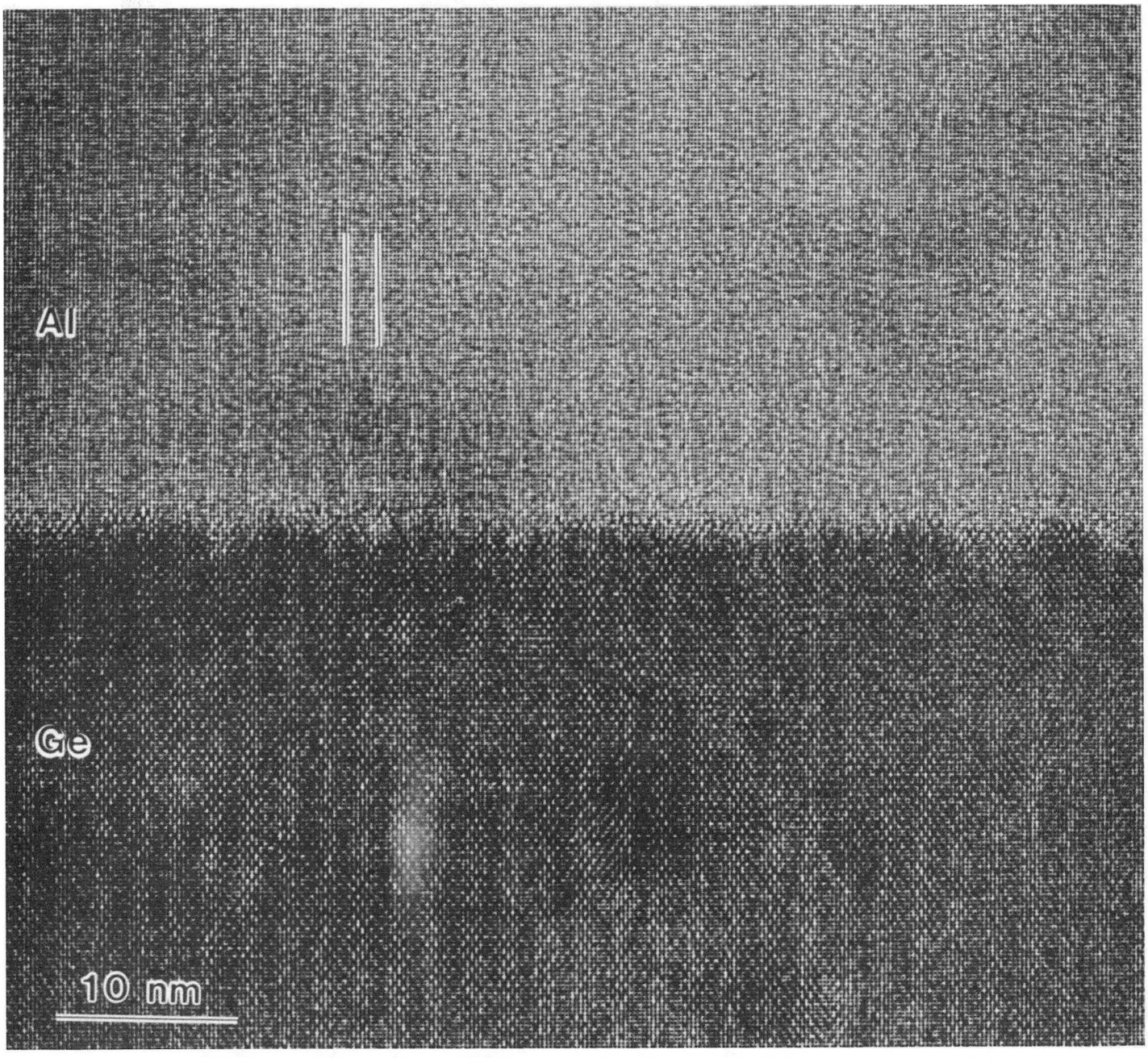

XBB 906-04596

Figure 8

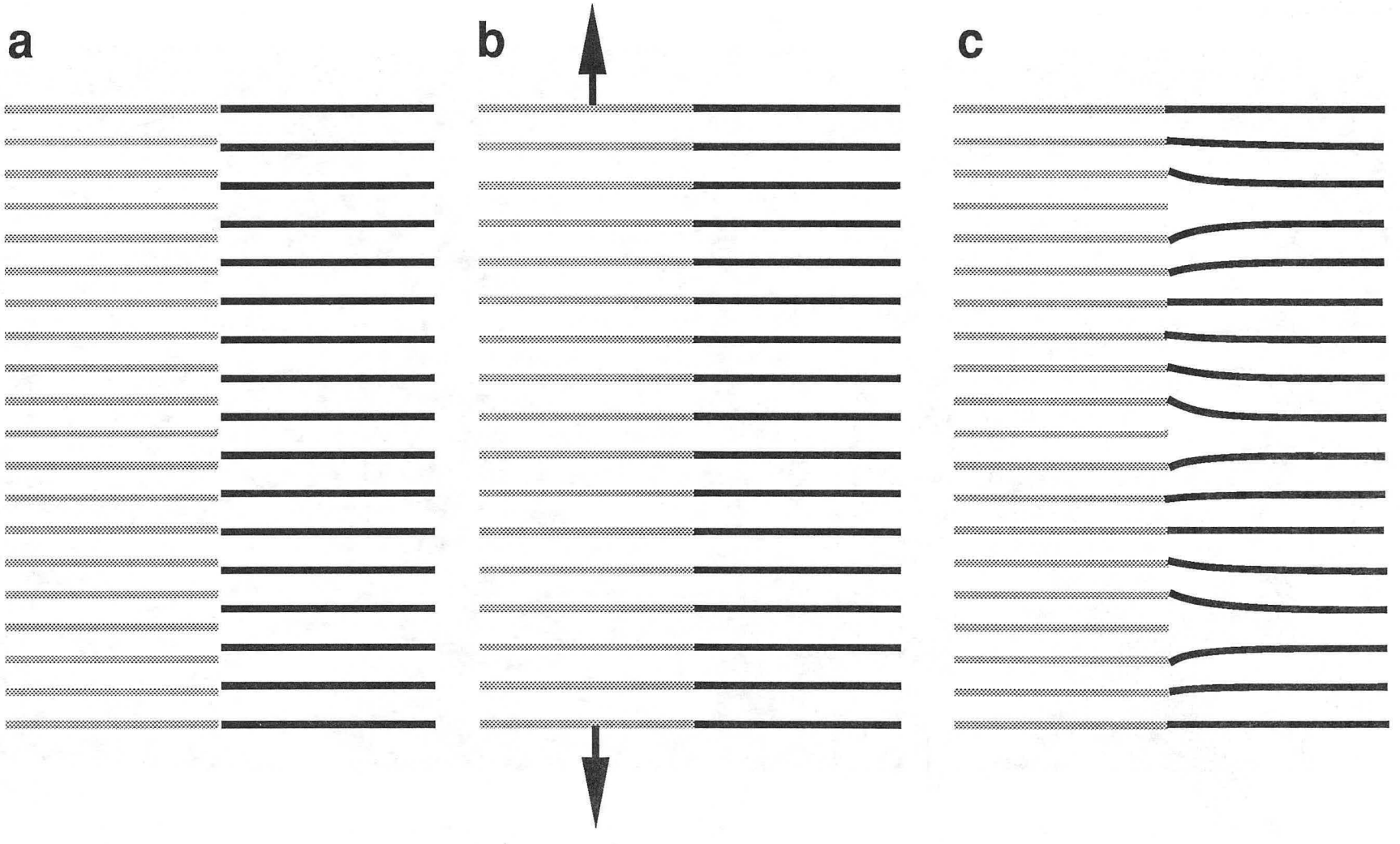

Figure 9

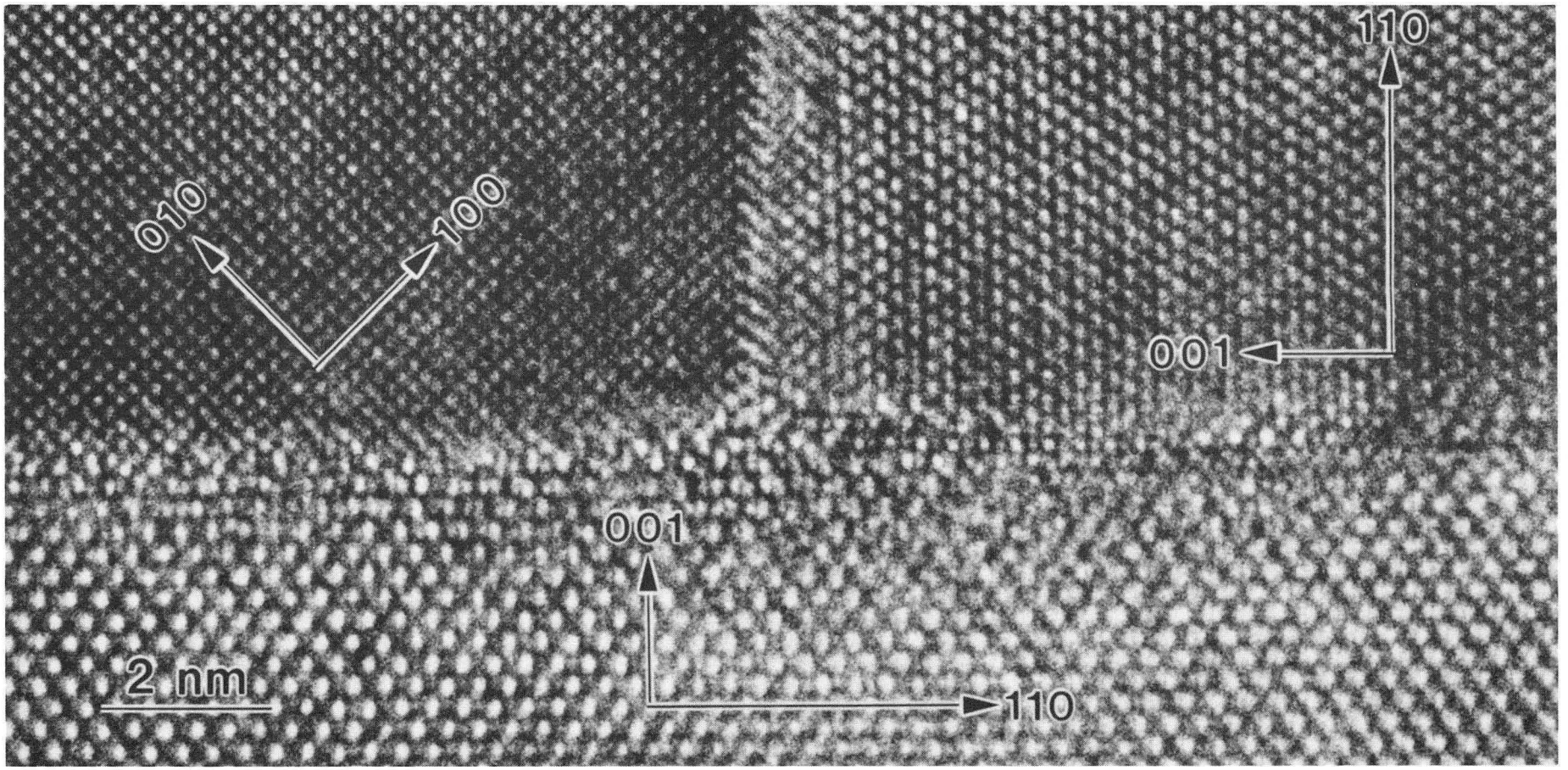

XBB 906-04595

Figure 10

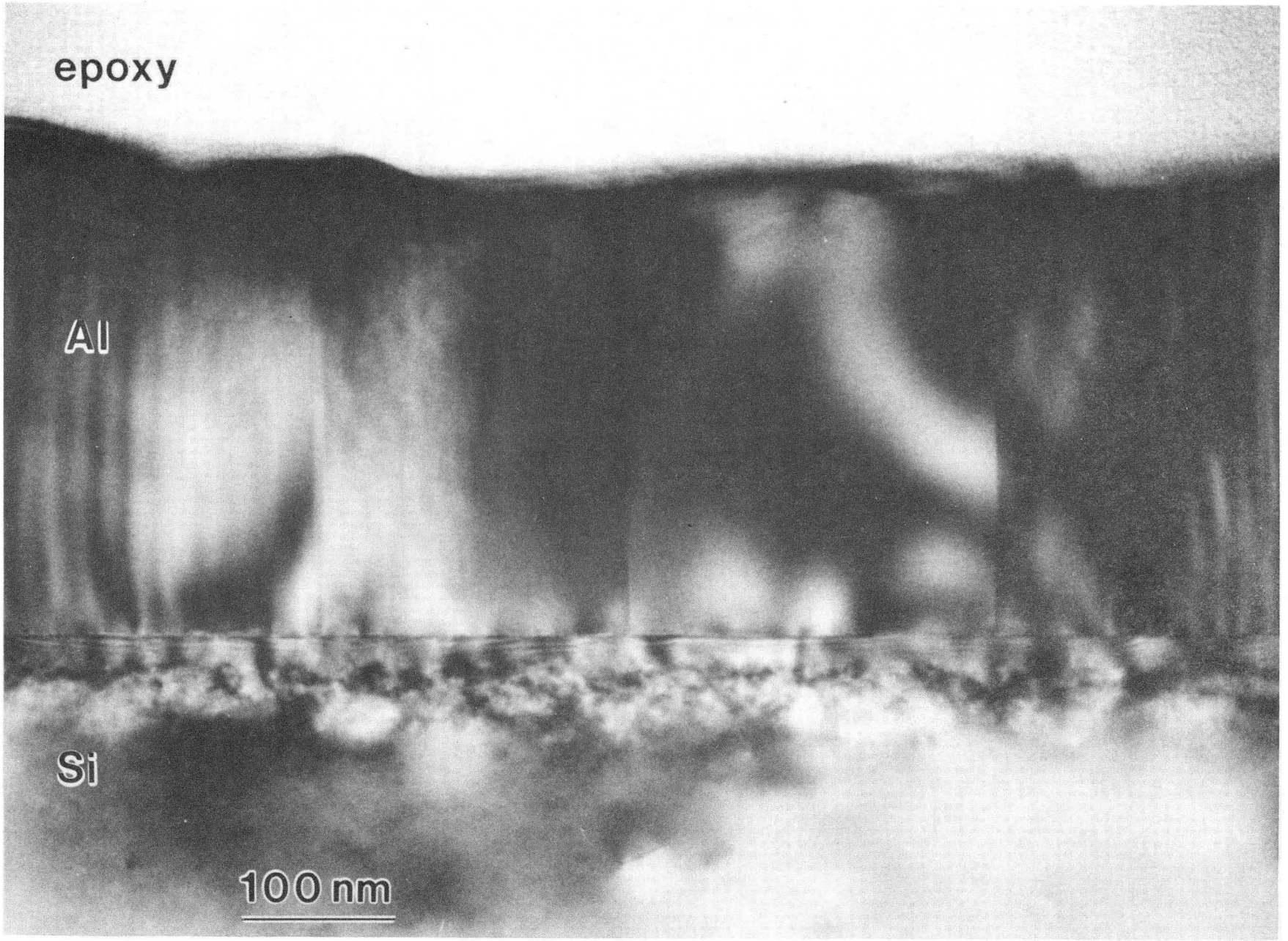

XBB 906-04594

Figure 11

LAWRENCE BERKELEY LABORATORY
UNIVERSITY OF CALIFORNIA
INFORMATION RESOURCES DEPARTMENT
1 CYCLOTRON ROAD
BERKELEY, CALIFORNIA 94720